

Lecture Notes

PH4202: Advanced Statistical Mechanics

Sabarno Saha

Email: ss22ms037@iiserkol.ac.in

Instructor: Prof. Bhavtosh Bansal

Date: 25 January 2026



"How do you want it—the crystal mumbo-jumbo or statistical probability?"

Table of Contents(By Topic)

1. Introduction	4
2. Van der Waals Equation of State	4
2.1. Molecular Interactions	4
2.2. Mean Field Treatment of Van der Waals Equation of State	5
2.3. Concavity of Entropy	9
2.4. Phase Coexistence Curves	12
2.5. Metastable States and Nucleation(†)	15
2.6. Transitions observed from Probability Distributions	17
3. Yang Lee Zeros	20
3.1. Theorems	20
3.1.1. No Phase Transition	23
3.1.2. Phase Transition	23
4. Magnetism	25
4.1. Ising Model	25
4.2. Mean Field Solution of the Ising Model	25
4.3. Partition Function	26
4.4. Critical Exponents and Behavior	27
4.5. Phase Diagrams and Hysteresis	27
4.6. Bragg-Williams Approximation	27
References	28

Table of Contents(By Lecture)

Lecture 1: Introduction and Van der Waals equation of state	4
Lecture 2: Convex Intruders and Phase transitions.	9
Lecture 3: Phase coexistence Curves and the Maxwell Construction.	12
Lecture 4: Yang-Lee zeros	20
Lecture 5: Critical exponents of the Van Der Waals Gas.	25
Lecture 6: Phase Transitions, Critical Exponents and Critical Opalescence.	25
Lecture 7: Introduction to Mean Field Ising Model	25

Lecture 1: Introduction and Van der Waals equation of state

1. Introduction

This course shall mainly focus on the statistical mechanics of equilibrium systems undergoing phase transitions. We shall only focus on classical systems in this course. So, without further ado, let us begin.

2. Van der Waals Equation of State

The ideal gas equation of state is given by

$$PV = Nk_B T \quad (2.1)$$

where P is the pressure, V is the volume, n is the number of moles of the gas, R is the universal gas constant and T is the temperature. This equation of state assumes that there are no interactions between the gas molecules and that the volume occupied by the gas molecules themselves is negligible compared to the volume of the container. In contrast to this, Johannes Diederick van der Waals proposed a more realistic equation of state for real gases, that can qualitatively explain the phase transition between water and gas. The Van der Waals equation of state is given by

$$\left(P + a \frac{N^2}{V^2} \right) (V - Nb) = Nk_B T \quad (2.2)$$

where a and b are constants that depend on the gas in question. Here, a accounts for the weak attractive interactions between the gas molecules, while b accounts for the finite size of the gas molecules. N is the number of molecules and k_B is the Boltzmann constant.

We shall be looking at how this equation of state is derived from a mean-field treatment of the system. Then we shall take a look at where this theory succeeds and where it fails. Before we proceed, let us first understand the nature of molecular interactions.

2.1. Molecular Interactions

To understand the behaviour of the real gas, we need to see how particles interact with each other. The most extensively studied potential of the pair-type potentials is the Lennard-Jones Potential(LJP). The form of the potential is given by,

$$u(r) = u_0 \left[\left(\frac{\sigma}{r} \right)^{12} - \left(\frac{\sigma}{r} \right)^6 \right] \quad (2.3)$$

where u_0, σ are constants that depend on the type of particles and $r = |r_i - r_j|$ is the inter-particle distance between two particles located at r_i and r_j respectively. The first term in the potential represents the repulsive interaction between the particles, while the second term represents the attractive interaction between the particles. The repulsive term dominates at short distances, while the attractive term dominates at long distances. The potential has a minimum at $r = r_m = 2^{\frac{1}{6}}\sigma$, which represents the equilibrium distance between two particles.

The exponent 12 is chosen for computational convenience,. The exponent 6 arises from the fact that the attractive interaction is due to dipole-dipole interactions, which decay as $\frac{1}{r^6}$. This can be derived by considering a particle with dipole moments p_1 separated by a distance r from another particle. There is an induced dipole moment p_2 in the second particle which can be assumed to be proportional to the field created by the first dipole moment at the location of the second particle. This gives us the r^{-6} decay of the attractive interaction.

Another commonly used potential is the hard-sphere potential, which considers a infinite potential when the particles are closer than a certain distance and the same as the attractive part of the Lennard-Jones potential when the particles are farther apart. The hard-sphere potential is given by,

$$u(r) = \begin{cases} \infty & r < r_0 \\ -u_0 \left(\frac{r_0}{r}\right)^6 & r \geq r_0 \end{cases} \quad (2.4)$$

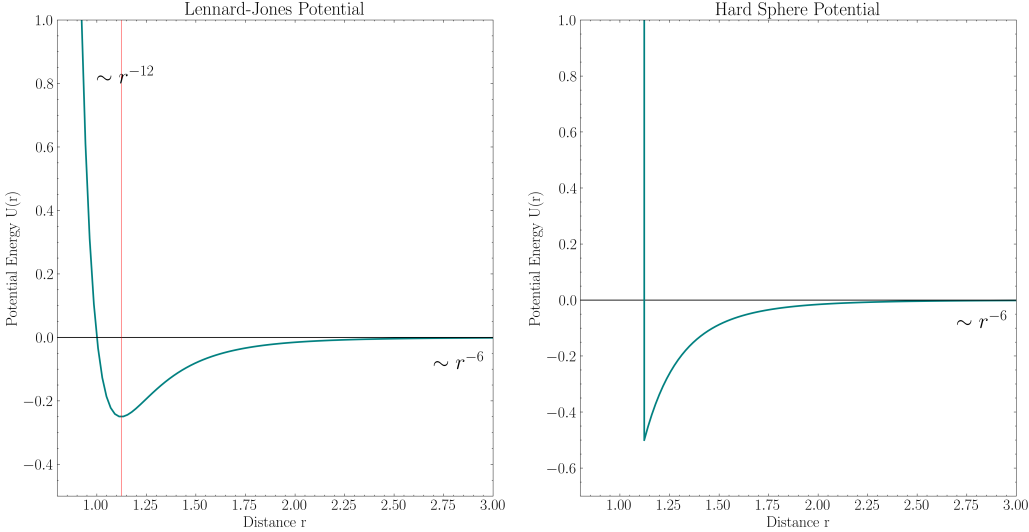


Figure 2: Lennard-Jones Potential and Hard-Sphere Potential

Generally, for systems in d dimensions, the repulsive part of the potential is taken to be r^{-n} where $n > d$ to ensure that the potential is short-ranged. If $n \leq d$, the potential is said to be long-ranged and special techniques are required to handle such systems.

2.2. Mean Field Treatment of Van der Waals Equation of State

One way of dealing with interactions added to a known Hamiltonian is to use perturbation theory. However, perturbations are defined continuously from a known system. This in general, cannot describe non-analytic changes in the system, such as phase transitions. Thus, we use an effective field approach, known as the mean-field theory. In this approach, we replace the effect of all other particles on a given particle with an average effect. This reduces the many-body problem to a single-body problem in an effective field. To illustrate this, let us derive the Van der Waals equation of state using mean-field theory.

The general Hamiltonian for a system of N particles interacting with each other,

$$H = \sum_{i=1}^N \frac{p_i^2}{2m} + U(r_1, r_2, \dots, r_N) \quad (2.5)$$

where p_i is the momentum of the i^{th} particle, m is the mass of the particles and $U(r_1, r_2, \dots, r_N)$ is the total potential energy of the system. For our case we shall use a pairwise potential, which means that the total potential energy can be written as,

$$U(r_1, r_2, \dots, r_N) = \frac{1}{2} \sum_{i \neq j} u(|r_i - r_j|) \quad (2.6)$$

Let us now consider the canonical partition function for this system,

$$Z = \left(\frac{1}{N!} h^{3N} \right) \int d^{3N}r \int d^{3N}p \exp(-\beta H) \quad (2.7)$$

where $\beta = \frac{1}{k_B T}$, h is some constant with the dimension of action and the factor $\frac{1}{N!}$ is included to account for the indistinguishability of the particles. The integral over the momenta can be performed easily, giving us,

$$Z = \left(\frac{1}{N!} \lambda^{-3N} \right) \int d^{3N} r \exp(-\beta U(r_1, r_2, \dots, r_N)) \quad (2.8)$$

where $\lambda = \frac{\hbar}{\sqrt{2\pi m k_B T}}$ is the thermal wavelength. Now, the integral over the positions is difficult to perform due to the presence of the potential energy term. Firstly, we can rewrite the potential energy term as an integral over the inter-particle distances, rather than a summation. To do this, define the density function as,

$$n(r) = \sum_{i=1}^N \delta(r - r_i) \quad (2.9)$$

The potential energy term can be written as,

$$\begin{aligned} U(\{|q_i - q_j|\}) &= \frac{1}{2} \sum_{i \neq j} u(|r_i - r_j|) \\ &= \frac{1}{2} \int d^3 r_1 \int d^3 r_2 n(r_1) n(r_2) u(|r_1 - r_2|) \end{aligned} \quad (2.10)$$

Here is where we make the mean-field approximation. We replace the density function $n(r)$ with its average value $n = \frac{N}{V}$, where V is the volume of the system. This approximation assumes that the density of particles is uniform throughout the system. With this approximation, the potential energy term becomes,

$$\begin{aligned} U &\approx \frac{1}{2} \int d^3 r_1 \int d^3 r_2 \left(\frac{N}{V} \right)^2 u(|r_1 - r_2|) \\ &= \frac{n^2}{2} \int d^3 r_1 \int d^3 r_2 u(|r_1 - r_2|) \end{aligned} \quad (2.11)$$

Since the potential $u(r)$ only depends on the distance between the particles, we can simplify the integral further by changing to relative coordinates. Define the new coordinates as,

1. The Centre of mass coordinate : $R = \frac{r_1 + r_2}{2}$
2. The relative coordinate : $r = r_1 - r_2$

Then the original coordinates can be expressed in terms of the new coordinates as,

1. $r_1 = R + \frac{r}{2}$
2. $r_2 = R - \frac{r}{2}$

The Jacobian of this transformation is ,

$$J = \left| \frac{\partial(r_1, r_2)}{\partial(R, r)} \right| = \left| \begin{pmatrix} 1 & \frac{1}{2} \\ 1 & -\frac{1}{2} \end{pmatrix} \right| = 1 \quad (2.12)$$

Using this transformation, the integral over the positions becomes,

$$\begin{aligned} \int d^3 r_1 \int d^3 r_2 u(|r_1 - r_2|) &= \int d^3 R \int d^3 r u(|r|) \\ &= V \int d^3 r u(r) \end{aligned} \quad (2.13)$$

where we have used the fact that the integral over the centre of mass coordinate R simply gives us a factor of the volume V . Thus, the potential energy term becomes,

$$U \approx \frac{n^2}{2} V \int d^3 r u(r) = \frac{N^2}{2V} \int d^3 r u(r) \quad (2.14)$$

The pair potential function used in this case is the hard-sphere potential defined in , except we use a general exponent s instead of 6 for the attractive part.

$$u(r) = \begin{cases} \infty & r < r_0 \\ -u_0 \left(\frac{r_0}{r} \right)^s & r \geq r_0 \end{cases} \quad (2.15)$$

Note that the potential is infinite when the particles are closer than r_0 . This causes a divergence in the integral over $r \in [0, r_0]$. This is very simply taken care of. Note that the Boltzmann factor $\exp(-\beta U)$ becomes zero when U is infinite. Thus, the region of integration where the potential is infinite does not contribute to the integral. Thus, we can simply change the limits of integration to $r \in [r_0, \infty)$. Thus, the integral becomes (using spherical symmetry),

$$\begin{aligned} \int d^3r u(r) &= \int_{r_0}^{\infty} 4\pi r^2 dr \left(-u_0 \left(\frac{r_0}{r} \right)^s \right) = -4\pi u_0 r_0^s \int_{r_0}^{\infty} r^{2-s} dr \\ &= \frac{4\pi u_0 r_0^3}{s-3} \end{aligned} \quad (2.16)$$

where we have assumed that $s > 3$ to ensure convergence of the integral. Thus, the potential energy term becomes,

$$U(\{|q_i - q_j|\}) \approx \frac{N^2}{2V} \frac{-4\pi u_0 r_0^3}{s-3} = a \frac{N^2}{V} \quad (2.17)$$

where $a = \frac{2\pi u_0 r_0^3}{s-3}$. Thus, the partition function becomes,

$$\begin{aligned} Z &= \left(\frac{1}{N!} \lambda^{-3N} \right) \int d^{3N}r \exp \left(\beta a \frac{N^2}{V} \right) \\ &= \left(\frac{1}{N!} \lambda^{-3N} \right) \exp \left(\beta a \left(\frac{N^2}{V} \right) \right) \int d^{3N}r \end{aligned} \quad (2.18)$$

The integral over the positions is not simply the volume to the power N because of the hard-sphere nature of the particles. The particles cannot come closer than a distance r_0 to each other. Consider adding in the particles one by one. The first particle can be placed anywhere in the volume V . The second particle can be placed anywhere in the volume V except for a sphere of radius r_0 around the first particle. Thus, the available volume for the second particle is $V - (\frac{4}{3})\pi(r_0)^3 = V - \Omega$, [cf. Figure 3]. Note that Ω is 8 times the volume of a particle. The distance of closest approach between two particles is r_0 , so the volume of each particle is considered to be a sphere of radius $\frac{r_0}{2}$.

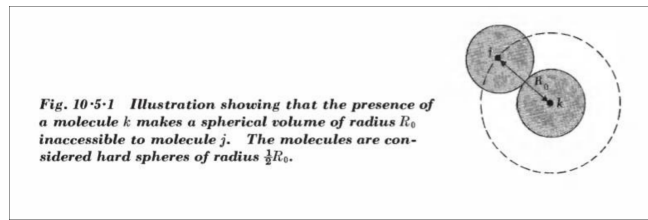


Figure 3: Excluded Volume for Hard-Sphere Particles. Source: [1]

$$\begin{aligned} \int d^{3N}r &\approx V(V - \Omega)(V - 2\Omega)\dots(V - (N-1)\Omega) \\ &= V^N \left(1 - \left(\frac{\Omega}{V} \right) \right) \left(1 - 2\left(\frac{\Omega}{V} \right) \right) \dots \left(1 - (N-1)\left(\frac{\Omega}{V} \right) \right) \\ &= V^N \left[\left(1 - \frac{\Omega}{V} \right) \left(1 - (N-1)\frac{\Omega}{V} \right) \right] \left[\left(1 - 2\frac{\Omega}{V} \right) \left(1 - (N-2)\frac{\Omega}{V} \right) \right] \dots \\ &\approx V^N \left(1 - \frac{N}{2} \frac{\Omega}{V} \right)^N \end{aligned} \quad (2.19)$$

To obtain the last line, we have paired the first and last terms, the second and second last terms and so on. This gives us $\frac{N}{2}$ pairs, each of which is approximately equal to $1 - N\frac{\Omega}{V}$ in the low density limit

where $N\frac{\Omega}{V} \ll 1$. In addition to that, the binomial approximation gives us the $\frac{1}{2}$ factor. We have also used that for large N , $(N - 1) \approx N$. Thus, the partition function becomes,

$$Z(T, V, N) = \left(\frac{1}{N!} \lambda^{-3N} \right) \exp \left(\beta a \frac{N^2}{V} \right) \left(V - \frac{N}{2} \Omega \right)^N \quad (2.20)$$

The free energy can be obtained from the partition function as,

$$\begin{aligned} F(T, V, N) &= -k_B T \log Z(T, V, N) \\ &= -k_B T \left[-\log N! + 3N \log \lambda + \beta a \frac{N^2}{V} + N \log \left(V - \frac{N}{2} \Omega \right) \right] \\ &= -k_B T \left[-N \log N + N + 3N \log \lambda + \beta a \frac{N^2}{V} + N \log \left(V - \frac{N}{2} \Omega \right) \right] \end{aligned} \quad (2.21)$$

where we have used Stirling's approximation $\log N! \approx N \log N - N$ for large N . The pressure can be obtained from the free energy as,

$$\begin{aligned} P &= -\frac{\partial F}{\partial V}_{T,N} = k_B T N \left[\frac{1}{V - \frac{N\Omega}{2}} \right] - a \frac{N^2}{V^2} \\ &\Rightarrow \left(P + a \frac{N^2}{V^2} \right) (V - Nb) = N k_B T \end{aligned} \quad (2.22)$$

where

$$a = \frac{2\pi u_0 r_0^3}{s-3} \quad ; \quad b = \frac{\Omega}{2} = \left(\frac{2}{3} \right) \pi r_0^3 \quad (2.23)$$

Note that b is four times the volume occupied by a particle. This is the Van der Waals equation of state. This equation of state can also be derived using other methods, such as the cluster expansion method, cf. [2]. Instead of using a mean field approximation, he expands out the Boltzmann factor of the interacting terms in powers of some function of density, giving us the virial expansion. He then truncates the series at the second virial coefficient. This gives the same result as the mean-field approximation.

Remark (Derivation): The Derivation is from "Fundamentals of Statistical and Thermal Physics" by F. Reif [1] under the alternate derivation of the Van der Waals Equation of state. However, there are some differences. Reif progresses in a different fashion compared to us. He first considers the hard-sphere potential to conclude that for each particle, an excluded volume V_x is present. This excluded volume is the volume around each particle where no other particle can enter due to the hard-sphere nature of the particles. Now he assumes in the available volume $V - V_x$, the potential is on an average constant. This is equivalent to our mean-field approximation, where we assumed the density to be uniform. He then goes on to find what V_x should be. However, his calculation makes an assumption less than ours.

He does not assume the dilute limit $\frac{N\Omega}{V} \ll 1$ to calculate the available volume for N particles. We place the particles one by one, and for each particle, we assume that the other $N - 1$ particles are already placed. Reif assumes that the particles are added simultaneously, which makes lesser sense to me. However, he does claim that his arguments are quite crude in nature.

Lecture 2: Convex Intruders and Phase transitions.

The van-der-waals equation of state is given by

$$\left(P + \frac{aN^2}{V^2} \right) (V - Nb) = Nk_B T \quad (2.1)$$

where a and b are constants specific to the fluid under consideration. This is a cubic equation in V for given values of P and T .

$$pV^3 - (Nk_B T + bP)V^2 + aN^2V - abN^3 = 0 \quad (2.2)$$

Given P and T , basically given an isotherm and an isobar, we can solve for the roots of this cubic equation to get the possible volumes of the system.

In the high temperature limit, the van der Waals equation reduces to the ideal gas law. However, at lower temperatures, we observe a glaring issue. For temperatures below a critical temperature T_c , the isotherms show an unstable behaviour. There is a region where the pressure increases with increase in volume, which is unphysical. Consider the pink line in Figure 9. The section of graph between points M and N is unphysical since $\frac{\partial P}{\partial V} > 0$ there. Let us see why this is unphysical.

The isothermal compressibility κ_T is defined as

$$\kappa_T = -\left(\frac{1}{V}\right)\left(\frac{\partial V}{\partial P}\right)_T \quad (2.3)$$

This is a response function that measures how much the volume changes with pressure at constant temperature. For a stable system, we must have $\kappa_T > 0 \implies \left(\frac{\partial V}{\partial P}\right)_T < 0$. This means that when we increase the pressure, the volume should decrease. Another way of observing this fact is to consider, particle number fluctuations in the grand canonical ensemble. The particle number fluctuations equal the isothermal compressibility times some positive factors. Thus, for a stable system, the particle number fluctuations must be positive, which again implies that $\kappa_T > 0$.

$$\frac{(\Delta N)^2}{\langle N \rangle^2} = k_B T \left(\frac{N}{V}\right) \kappa_T \quad (2.4)$$

The uninterested reader can refer to [3] for a detailed discussion on this topic. Thus, the region between M and N in Figure 9 is unphysical. Before we try to fix this issue, let us obtain the instability picture from the entropy perspective.

2.3. Concavity of Entropy

A stable equilibrium state must be a state of maximum entropy. If we can convince ourselves that the entropy is concave in its natural variables, we can use this property to identify unstable regions. Let us follow the approach by [4] to show, at least heuristically, that entropy is concave in its natural variables.

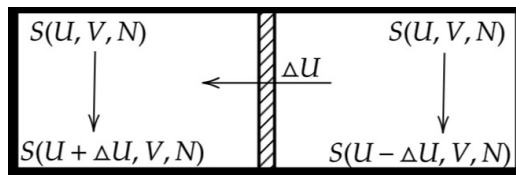


Figure 4: Callen illustration of entropy exchange between two subsystems.

Source: [5].

Consider an isolated system made up of two identical subsystems 1 and 2, separated by a rigid adiabatic wall. The total energy, volume and particle number of the combined system are fixed. Then the fundamental equation of the subsystems is $S = S(U, V, N)$. Consider removing energy ΔU from

subsystem 2 and giving it to subsystem 1. The initial entropies of the two subsystems are $S(U_1, V, N)$ and $S(U_2, V, N)$. After the energy exchange, the entropies become $S(U_1 + \Delta U, V, N)$ and $S(U_2 - \Delta U, V, N)$. Let us now allow the adiabatic wall to be transformed to a diathermal wall, allowing heat exchange between the two subsystems. Suppose now that the entropy varies with energy as shown in Figure 5. One can see that $S(U_1 + \Delta U, V, N) + S(U_2 - \Delta U, V, N) \geq 2S(U, V, N)$. One would see that the energy flows from one subsystem to another spontaneously. One would also see this happening in regions within the subsystem. Thus, the system would remain in an inhomogenous state, which is the hallmark of a phase transition. However, if the entropy is concave in energy, we have $S(U_1 + \Delta U, V, N) + S(U_2 - \Delta U, V, N) \leq 2S(U, V, N)$. Thus, the system would evolve to a homogenous state with equal energies in both subsystems.

Thus for stable systems, the entropy must be concave in its natural variables, which leads us to the stability criteria(a property of concave functions).

$$\left(\frac{\partial^2 S}{\partial U^2} \right)_{V,N} \leq 0 \quad (2.5)$$

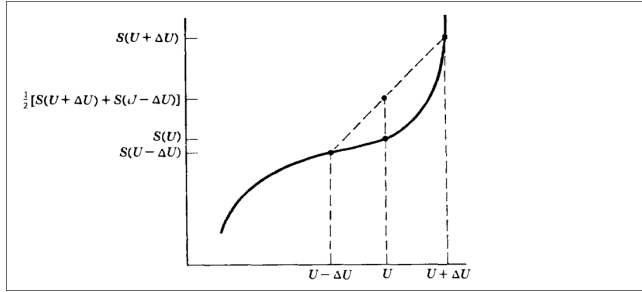


Figure 5: Convex intruder in entropy. “Convex Intruders” are places of convexity often signalling phase transitions. These are used to study phase transitions in mesoscopic systems. Image Source: [4].

This stability criteria can be further generalized to other variables like (V, N) . Now consider a similar scenario but with moving the rigid wall to one of the sides. Then, allow the wall to move. Then a similar argument would lead us to the conclusion that

$$\left(\frac{\partial^2 S}{\partial V^2} \right)_{U,N} \leq 0 \quad (2.6)$$

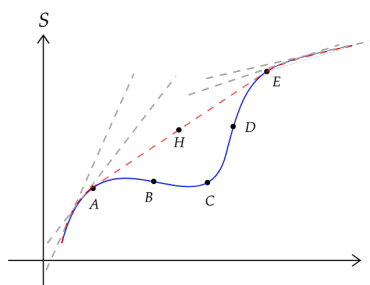


Figure 6: Convex Intruder in fundamental equation plot. Here, the entropy has a convex region between points A and B . This convex region is unphysical since it violates the concavity condition of entropy. Source: [5]

How do we resolve this issue of intruders in entropy? The stable thermodynamic fundamental equation is then obtained from this “underlying fundamental equation” by the constructing tangents. This construction is called the concave envelope construction. The concave envelope is the smallest concave function that lies above the underlying function. The family of tangents that lie above the underlying function are drawn(called the *superior tangents*). The concave envelope is then the envelope of these superior tangents. It is of note that we also obtain metastable states, whenever a convex intruder is present. We shall discuss this later in the context of nucleation in first order phase transitions. The lines BC and CD are locally stable but globally unstable. BCD is an unstable region.

We can translate these stability conditions to other free energies as well. We can use the Legendre transforms to obtain other free energies. For example, the Helmholtz free energy is given by $F = U - TS$. The natural variables of F are (T, V, N) . We can then see that,

$$\begin{aligned} F &= U - TS \\ dF &= -S \, dT - P \, dV + \mu \, dN \end{aligned} \quad (2.7)$$

Then we have,

$$\frac{\partial S}{\partial T} = -\left(\frac{\partial^2 F}{\partial T^2}\right)_{T,N} = \frac{C_v}{T} \geq 0 \quad (2.8)$$

Similarly, we get,

$$\frac{\partial^2 F}{\partial V^2} = -\left(\frac{\partial P}{\partial V}\right)_{T,N} = \frac{\kappa_T}{V} \geq 0 \quad (2.9)$$

Thus, the stability conditions in terms of Helmholtz free energy are,

$$\left(\frac{\partial^2 F}{\partial T^2}\right)_{V,N} \leq 0 \quad \left(\frac{\partial^2 F}{\partial V^2}\right)_{T,N} \geq 0 \quad (2.10)$$

The stability for other free energies can be obtained in a similar manner [4], [6].

$$\begin{array}{ll} \left(\frac{\partial^2 G}{\partial T^2}\right)_{P,N} \leq 0 & \left(\frac{\partial^2 G}{\partial P^2}\right)_{T,N} \geq 0 \\ \left(\frac{\partial^2 H}{\partial S^2}\right)_{P,N} \leq 0 & \left(\frac{\partial^2 H}{\partial P^2}\right)_{S,N} \geq 0 \end{array} \quad (2.11)$$

Since all of these functions are related by Legendre transforms, without using the thermodynamic relations, we can obtain these from the properties of Legendre transforms. In general for constant N , the legendre transforms of Energy are concave in their extensive variables and convex in their intensive variables. We can now observe typical phase transition behaviour in different free energy functional curves.

These stability conditions along with construction of concave envelopes can be used to resolve the van der Waals instability. From the graph of the Van der waals equation of state, we can find the graphs of the free energies. Then we could apply the same principles to obtain the stable free energy curves.

One also needs to discuss about the Legendre transform of energy or entropy. The Legendre transforms give us the free energy functionals along with ensemble equivalence. Legendre transforms in thermodynamics translate to laplace transforms in statistical mechanics. A detailed discussion on this topic can be found later.

Lecture 3: Phase coexistence Curves and the Maxwell Construction.

2.4. Phase Coexistence Curves

The Helmholtz free energy and the Gibbs free energy are related by a Legendre transform. Given any potential, we can obtain other potentials by Legendre transforms. Let's see an example with the Helmholtz and Gibbs free energies.

The Gibbs free energy is defined as,

$$\begin{aligned} G &= F + PV = U - TS + PV \\ dG &= -S dT + V dP + \mu dN \end{aligned} \quad (2.1)$$

The natural variables of G are (T, P, N) . Thus, we have,

$$\begin{aligned} S &= -\left(\frac{\partial G}{\partial T}\right)_{P,N} \\ V &= \left(\frac{\partial G}{\partial P}\right)_{T,N} \end{aligned} \quad (2.2)$$

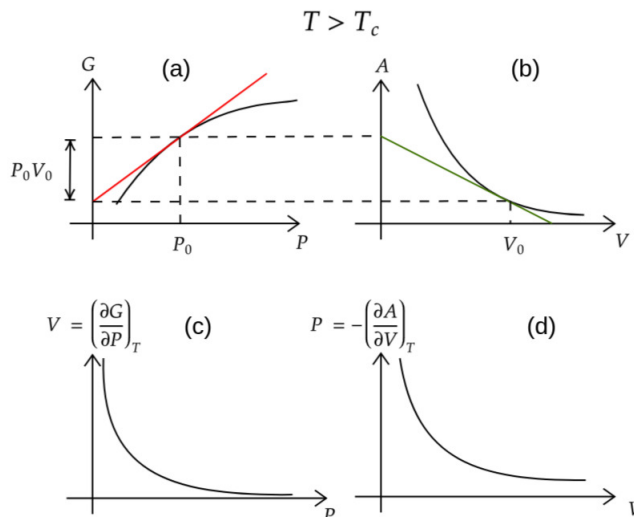


Figure 7: Relations between Helmholtz free energy, Gibbs free energy, Volume and Pressure. The plots are done for a temperature above the critical temperature. These are example curves which look similar to ideal gas curves. In this convention, F would be convex if G is concave. Also note that A here is helmholtz free energy, which is denoted by F in the notes. Source: [5].

Consider the Gibbs free energy vs pressure plot at constant temperature shown in Figure 7. We see that for each temperature, there is a unique Gibbs free energy value for each pressure. This is true for temperatures above the critical temperature. The volume can be obtained from the slope of these curves. The stability conditions for Gibbs free energy dictate that G should be concave in pressure P . Since the function is concave everywhere, the volume is an injective function of pressure. We can then invert the function to obtain $P = P(T, V)$. We can also obtain the Helmholtz free energy from the Gibbs free energy by calculating $F(V_0) = G(P_0) - P_0 V_0$. As a result of these, we establish similar diagrams for Gibbs free energy $G(P)$, Helmholtz free energy $F(V)$, $V(P)$ and $P(V)$.

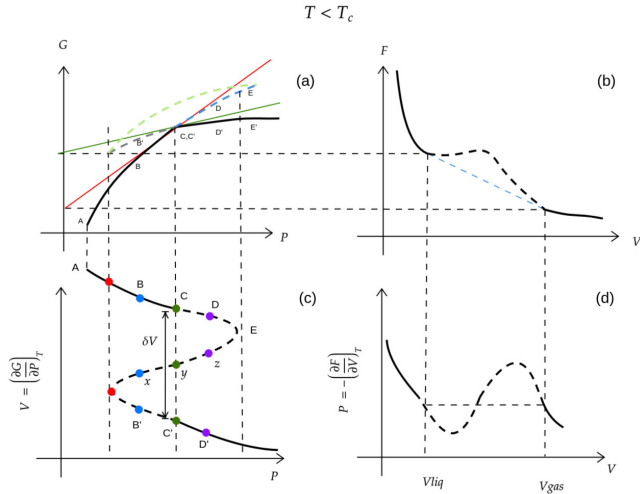


Figure 8: Relations between Helmholtz free energy, Gibbs free energy, Volume and Pressure. The plots are done for a temperature below the critical temperature. Since the Gibbs free energy becomes multivalued, the Volume as a function of temperature(when calculated pointwise from the Gibbs Free energy) fails the vertical line test for a function.

Source: [5].

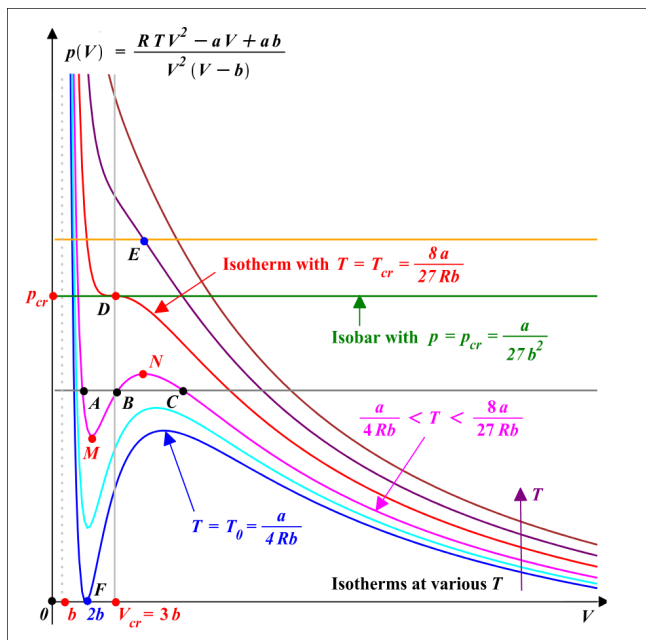


Figure 9: The graphical solution of the van der Waals equation of state. Note that when $T \gg 1$, we obtain the ideal gas limit and similar isotherms. Note that under the isotherm $T < T_c$, there are three possible volumes for a given pressure. This cubic form of the equation also indicates that there must be a critical point where the three roots merge into one. Later, on as we shall observe that Maxwell construction also imposes a constraint relation between P and T . A very nice discussion regarding the properties and how the maxwell construction gives rise to phases from a purely mathematical perspective is given in [7].

For temperatures below the critical temperature, the Gibbs free energy vs pressure plot looks like Figure 8. We see that the P versus V plot looks like the van der Waals isotherm with the unphysical region between points M and N in Figure 9. The multivaluedness of the Gibbs free energy manifests itself as an instability in the Helmholtz free energy vs volume plot. The Helmholtz free energy becomes concave in a certain region, violating the stability conditions. We can again use the concave envelope construction to obtain the stable Helmholtz free energy curve. However, instead of constructing the concave envelope, we shall create a convex envelope for the Helmholtz free energy. This is because the Helmholtz free energy is convex in volume for stable systems. Since the pressure is given by $P = -(\frac{\partial F}{\partial V})_{T,N}$, the slope of the Helmholtz free energy vs volume plot for the convex envelope construction would give us the flatline in the P versus V plot, which is the Maxwell construction, in the region between points M and N in Figure 9. This can be seen as the isobar passing through the points A and C .

Another constraint that the Maxwell construction imposes is that the areas of the two regions, AMB and BNC in Figure 9 must be equal. Consider the cycle $AMBNCA$. The work done in this cycle is given by,

$$\oint PdV = \oint TdS - \oint dU = 0 \quad (2.3)$$

where the last equality follows from the fact that U and S are state functions. Thus, the work done in the cycle must be zero. Thus the areas of the two regions must be equal.

During the maxwell construction, the lowest Gibbs free energy branch is chosen as the stable branch. This is so because in the legendre transform convention we follow, the maximum entropy principle translates to the minimum Gibbs free energy principle. Thus, during the phase transition, the system jumps from one branch of the Gibbs free energy curve to another branch with lower Gibbs free energy. This also relates to superheating and supercooling phenomena, which is related to the phenomenon of nucleation in first order phase transitions. We shall discuss this later.

Let's discuss what happens physically during this phase transition, from the graphs. Note that the van der Waals equation of state is a cubic equation in V for given values of P and T . Thus given an isobar and an isotherm, we can solve for the roots of this cubic equation to get the possible volumes of the system. For temperatures below the critical temperature, there are three roots for a given pressure in the region between points M and N in Figure 9. We should also note that fixing an isobar also fixes the isotherm, since the two are related by equal areas in the Maxwell construction. Thus, given P and T , we obtain phase transitions due to the cubic nature of the equation of state. Basically if we follow the gibbs free energy vs pressure plot. As we decrease pressure, we transition from one branch to another branch of lower gibbs free energy, which corresponds to a jump in volume. This jump in volume is the phase transition from liquid to gas. The reverse happens when we increase pressure, leading to gas to liquid phase transition.

If we use the Gibbs Free energy graph vs T , we shall also obtain a discontinuity in entropy. This can be related to the latent heat of vaporization during the liquid to gas phase transition. In modern notation a first order phase transition is called an *abrupt* phase transition, since the first derivatives of the Gibbs free energy are discontinuous during the phase transition and abruptly change. In higher order phase transitions, higher derivatives of the Gibbs free energy are discontinuous. During abrupt phase, one needs to provide extra latent heat $T\delta S$ to change the phase of the system at constant temperature and pressure. This is exactly the jump in entropy seen in Figure 10. Higher order phase transitions do not involve latent heat, since entropy remains continuous during such phase transitions. However, higher derivatives are discontinuous.

Another signature of first order phase transitions is nucleation and metastability. We shall discuss these phenomena in the next section.

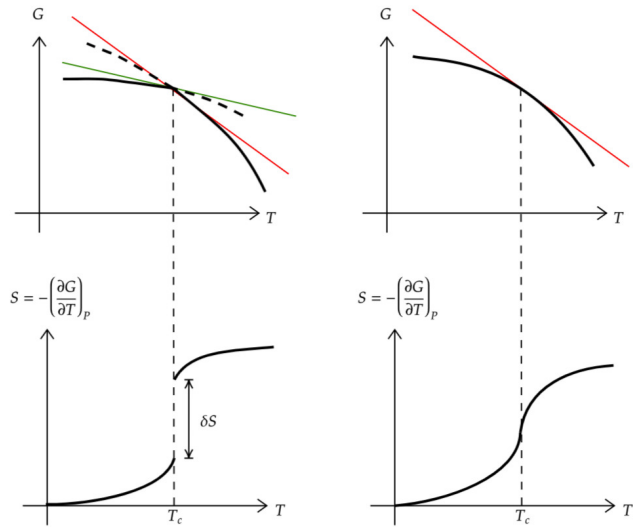


Figure 10: Gibbs free energy vs Temperature plot showing discontinuity in entropy during phase transition. Source: [5].

2.5. Metastable States and Nucleation(\dagger)

During the concave envelope construction, we also obtain metastable states. These are states which are locally stable but globally unstable. We shall understand metastable states and nucleation in the context of liquid to gas phase transition.

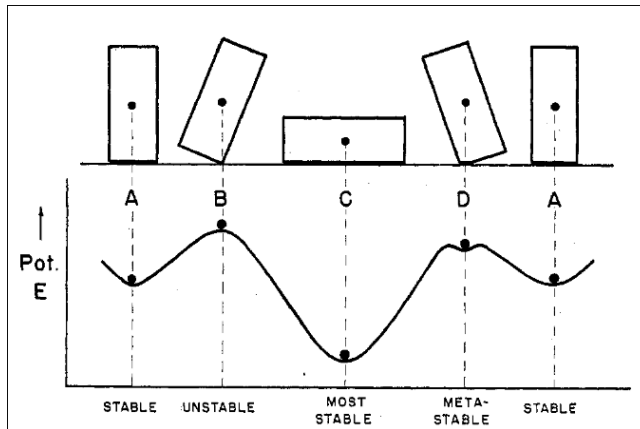


Figure 11: A schematic representation of stable, metastable and unstable states. The ball represents the state of the system. The valleys represent stable and metastable states, while the hill represents unstable states. Source: [8].

Consider a brick like in Figure 11. The brick can be in multiple states. A is a locally stable state, B is an unstable state and C is a globally stable state. Suppose we flatten out a corner of the brick in configuration B. We obtain the brick in configuration D. This is a metastable state. The difference between unstable and metastable states is that in unstable states, any small perturbation would drive the system away from that state. However, in metastable states, small perturbations would not drive the system away from that state. A finite perturbation is required to drive the system away from a metastable state. In this context, the strength of the perturbations decide the stability between metastable and locally stable states. We can consider them to be similar.

Continuing in a similar vein, in Figure 9, AM and NC are locally stable regions, which represent supercooled and superheated states respectively. This can bee seen from a plot of Gibbs free energy vs volume.

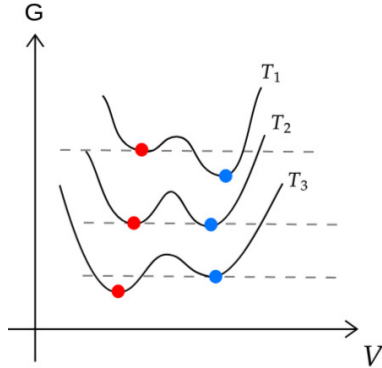


Figure 12: The gibbs free energy gives us two minimas near the phase transition point. There will be one minima of the liquid phase(the red point) over a certain range of temperatures we still get two minimas and at higher temperatures depth of the minimas changes. Source: [5].

In Figure 12, we see that there are two minimas in the Gibbs free energy vs volume plot. The left minima corresponds to the liquid phase and the right minima corresponds to the gas phase. As we decrease temperature, the depth of the left minima increases, making it the globally stable state. However, the right minima still exists as a locally stable or a metastable state. This metastable state corresponds to supercooled gas. The system might still exist in this supercooled gas state, until a finite perturbation or fluctuations in the system drive it to the globally stable liquid state. This process of nucleation is often observed in first order phase transitions. A nice discussion regarding nucleation is given in [8].

In one phase, nearby phase transitions, an embryo of the other phase can form due to fluctuations. For example, in gas, small droplets of liquid can form due to fluctuations. Formation of these droplets causes lower gibbs free energy as we observe from the graphs. However, this incurs another energetic cost due to surface tension. The theory of nucleation answers a really important question. When does water boil? Consider a spherical droplet of radius r of liquid forming in the gas phase. The change in energy due to the formation of this droplet is given by,

$$\Delta E = -\left(\frac{4}{3}\right)\pi r^3 \Delta g + 4\pi r^2 \gamma \quad (2.4)$$

where Δg is the difference in Gibbs free energy density between the two phases and γ is the surface tension. The first term is the volume term, which favours droplet formation, while the second term is the surface term, which discourages it. So fluctuations can create droplets, which die down due to energetic cost of surface tension. However larger and larger droplets can form due to fluctuations. There is a critical radius r_c beyond which the droplets grow spontaneously, leading to phase transition. This is how fluctuations drive nucleation and cause a phase transition. This is why supercooled liquid, on received a finite perturbation, can transition to the globally stable phase.

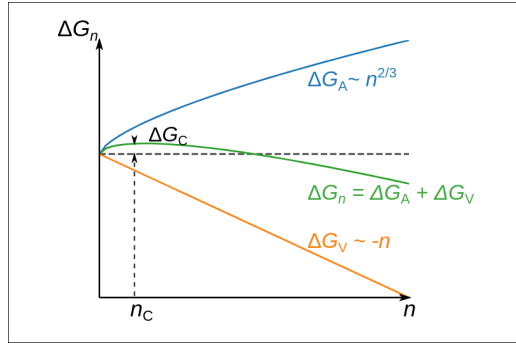


Figure 13: Change in Gibbs free energy due to formation of a droplet of radius r in the metastable phase. There is a critical radius r_c beyond which the droplet grows spontaneously, leading to phase transition. Considering the brick analogy, the green line is a zoomed out version of D state of the brick. Source: [9]

We can also see that the nucleation process is related to the concave envelope construction. The concave envelope construction gives us the globally stable states. However, during the construction, we also obtain metastable states. These metastable states correspond to supercooled and superheated states in liquid to gas phase transitions. The nucleation process drives the system from these metastable states to the globally stable states. The supercooling and superheating phenomena result in interesting hysteresis curves.

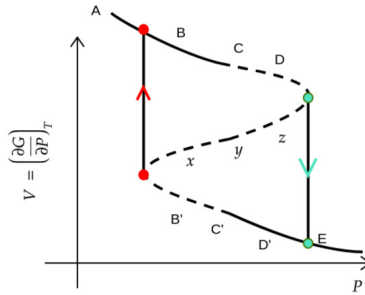


Figure 14: Hysteresis curve during liquid to gas phase transition. The blue curve corresponds to heating while the red curve corresponds to cooling. The hysteresis is due to superheating and supercooling phenomena. Source: Modified from [5].

One can also observe these phase transitions from the probability interpretation of partition functions. We follow Kardar [2] in this regard.

2.6. Transitions observed from Probability Distributions

The free energy is related to the partition function by,

$$F = -k_B T \ln Z \quad (2.5)$$

To this note let us observe something. Consider $\Omega(E)$ to be the number of microstates with energy E . Then let us define the Laplace transform of $\Omega(E) = \int d\Gamma \delta(H - E)$ where H is the hamiltonian, as,

$$Z(\beta) = \int dE \quad \Omega(E) \exp(-\beta E) = \int d\Gamma \exp(-\beta H) \quad (2.6)$$

where $\beta = \frac{1}{k_B T}$. This is the canonical partition function. This completes a transformation from the microcanonical ensemble to the canonical ensemble. Note that the relation to thermodynamics is given by the Boltzmann relation,

$$S(E) = k_B \ln \Omega(E) \quad (2.7)$$

The connection to thermodynamics in the canonical ensemble is given by,

$$\mathcal{F}(\beta) = \beta E(\beta) - \mathcal{S}(E(\beta)) \quad (2.8)$$

where $\mathcal{F}(\beta) = \beta F(\beta)$ and $\mathcal{S}(E) = \frac{S(E)}{k_B}$, which is a legendre transform pair.

Remark (Legendre Transform(†)):

There are two conventions for Legendre transforms cf [10]. One transforms convex functions to convex functions and the other transforms convex functions to concave functions. If we follow the first convention, we have,

$$\mathcal{F}(\beta) = \beta E(\beta) - \mathcal{S}(E(\beta)) \quad [(\mathcal{F}, \beta) \Leftrightarrow (\mathcal{S}, E)] \quad (2.9)$$

This converts convex functions to convex functions. This definition is contrary to what is used in thermodynamics. However, this convention has one very nice feature. The legendre transform is an involution in this convention. That is, applying the legendre transform twice gives us back the original function. That is, the Legendre transform is its own inverse.

If we follow the second convention, we have,

$$F(T) = E(S) - TS(E(T)) \quad [(F, T) \Leftrightarrow (E, S)] \quad (2.10)$$

This converts convex functions to concave functions and vice versa. This convention is followed in Sagnik's lecture notes [5].

One can refer to [10] for a detailed discussion regarding these two conventions. One can also refer to [11] for an excellent discussion regarding Legendre transforms, its geometric interpretation and its applications in thermodynamics. It also discusses the conversion of laplace transforms in statistical mechanics to legendre transforms in thermodynamics.

The connections of Legendre transforms to statistical mechanics is quite important. It determines what free energy functional should we use to determine our thermodynamic properties. For example, in the canonical ensemble, we use the Helmholtz free energy since the natural variables are (T, V, N) . In the grand canonical ensemble, we use the grand potential since the natural variables are (T, V, μ) . This is done, because we cannot control energy in the canonical ensemble, but we can control temperature. Similarly, in the grand canonical ensemble, we cannot control particle number, but we can control chemical potential. So we legendre transform out the energy to get the correct free energy functional for the canonical ensemble and also legendre transform out the particle number to get the correct free energy functional for the grand canonical ensemble.

We should also note that in the involutive convention, the natural variables come out to be β . When we go to grand canonical ensemble, the natural variables come out to be β and $\eta = -\beta\mu$, as we shall see later. These are infact the Lagrange multipliers that appear during the maximization of entropy with constraints on average energy and average particle number.

Again we can go from the canonical ensemble to the grand canonical ensemble by taking a discrete Laplace transform with respect to particle number N . The grand canonical partition function is given by,

$$\mathcal{Z}(T, V, N) = \sum_{N=0}^{\infty} \exp(\beta\mu N) Z(T, V, N) \quad (2.11)$$

Similarly, the connection to thermodynamics is given by,

$$\Phi = U - TS - \mu N \quad (2.12)$$

where $\Phi = -k_B T \ln \mathcal{Z}$ is the grand potential.

Remark (Grand potential(\dagger)): Just for the fun of it, we can find the legendre transform relation between grand potential and entropy in the involutive form. We have,

$$\Phi(\beta, \eta) = \beta E(\beta, \eta) + \eta N(\beta, \eta) - \mathcal{S}(E(\beta, \eta), N(\beta, \eta)) \quad (2.13)$$

where $\eta = -\beta\mu$, $\Phi = \beta\Phi$ and $\mathcal{S} = \frac{S}{k_B}$. This is again a legendre transform pair $(\Phi, \beta, \eta) \iff (\mathcal{S}, E, N)$. Note that this convention also corrects the sign of the exponent in the discrete laplace transform.

$$\mathcal{Z}(T, V, N) = \sum_{N=0}^{\infty} \exp(-\eta N) Z(T, V, N) \quad (2.14)$$

We can also see the Laplace transform from canonical to the grand canonical ensemble by legendre transforming \mathcal{F}

$$\Phi(\beta, \eta) = \eta N(\beta, \eta) - \mathcal{F}(\beta, N(\beta, \eta)) \quad (2.15)$$

The equation of state for the grand canonical ensemble is given by,

$$\beta PV = \ln \mathcal{Z}(T, V, \mu) = \ln \left(\sum_{N=0}^{\infty} \exp(V\psi(n)) \right) \quad (2.16)$$

where

$$\psi(n) = n \ln \left(n^{-1} - \frac{\Omega}{2} \right) + \beta an^2 + \Delta n \quad (2.17)$$

and $n = \frac{N}{V}$ is the number density and $\Delta = 1 + \beta\mu - \ln(\lambda^3)$, where λ is the thermal wavelength. Here, a is a constant from the van der Waals equation of state. Since in the thermodynamic limit, $V \rightarrow \infty$, we can use the saddle point approximation to evaluate the sum. The saddle point approximation states that for large V ,

$$P_{\text{g.c.}} V = k_B T V \psi(n^*) \quad (2.18)$$

where n^* is the value of n which maximizes $\psi(n)$. Here, we have denoted the pressure to be the grand canonical pressure. Generally, since the ensembles are equivalent, the grand canonical pressure is equal to the canonical pressure.

The densities n_α maximizing $\psi(n)$ satisfy,

$$\begin{aligned} \left. \left(\frac{\partial \psi}{\partial n} \right) \right|_{T, \mu} &= 0 \\ \Rightarrow \Delta &= -\ln \left(n_\alpha^{-1} - \frac{\Omega}{2} \right) + \frac{1}{1 - n_\alpha \Omega / 2} - 2\beta a n_\alpha \end{aligned} \quad (2.19)$$

This equation admits multiple solutions for n_α near the phase transition point. However, In the thermodynamic limit, the system chooses the density n^* which maximizes $\psi(n)$. So when there are multiple solutions, the maximum contribution comes from the density which gives the highest value of $\psi(n)$. In that case the grand canonical pressure is equal to the canonical pressure at that density. This formalism serves to augment our previous graphical discussion regarding phase transitions.

Suppose we have two peaks near the phase transition point. The two densities n_{liq} and n_{gas} correspond to the two phases. The phase transition occurs when the two peaks have the same height. As we vary temperature and pressure, the heights of the two peaks change. At the phase transition point, the two peaks have the same height. We denote this point with the temperature T^* . Since we take the thermodynamic limit, the system jumps from one peak to another peak as we cross the phase

transition point. This jump corresponds to the phase transition from liquid to gas. This is how phase transitions can be observed from the probability distributions in statistical mechanics. This complete derivation is given in [2]. As a result we obtain

$$\ln \mathcal{Z} = \lim_{V \rightarrow \infty} \ln(e^{\beta V P_{\text{liq}}} + e^{\beta V P_{\text{gas}}}) = \begin{cases} \beta V P_{\text{liq}} & \text{if } T > T^* \\ \beta V P_{\text{gas}} & \text{if } T < T^* \end{cases} \quad (2.20)$$

As an end to this lecture on phase coexistence curves and Maxwell construction, we arrive at a rather remarkable conclusion.

Theorem 2.6.1 (Phase transitions): There are no phase transitions in finite systems.

We observed a specific case here. The general heuristic argument is as follows. In finite systems, the partition functions are sums of individual microstate probabilities, which are analytic in their parameters. As a result, the free energies are also analytic in their parameters. However, phase transitions are marked by non-analyticities in free energies. Thus, phase transitions can only take place in infinite systems, where taking some sort of limit can lead to non-analyticities in free energies.

In finite systems, we observe what are called *crossovers*. Instead of abrupt jumps in thermodynamic quantities, we observe smooth transitions. However, as we take the thermodynamic limit, these crossovers become sharper and sharper, leading to non-analyticities in free energies and abrupt phase transitions.

Lecture 4: Yang-Lee zeros

3. Yang Lee Zeros

In a seminal work in 1952 [12], [13], C.N. Yang and T.D. Lee developed a theory to understand phase transitions in terms of the zeros of the partition function in the complex plane.

Let us again consider the grand canonical partition function for a system of particles, with a bath at temperature T and fugacity $z = \exp(\beta\mu)$.

$$\mathcal{Z}(T, V, \mu) = \sum_{N=0}^{\infty} z^N \mathcal{Z}(T, V, N) \quad (3.1)$$

Similar to the case of van der Waals gas, if we impose the constraint that the particles have a finite size, then there is a maximum number of particles N_{\max} that can be accommodated in the volume V . This means that the sum above is finite, and hence \mathcal{Z} is a polynomial in z of degree N_{\max} . Thus this polynomial shall, in general, have N_{\max} complex roots $z_1, z_2, \dots, z_{N_{\max}}$. The phase transitions can be observed in the non-analyticity of the grand partition function, of the form $\ln(\mathcal{Z})$. This non-analyticity can arise when one (or more) of the roots z_i approaches the positive real axis in the thermodynamic limit. Then, we get a singularity in $\ln(\mathcal{Z})$ for a physically realizable value of z , leading to a phase transition. Let's formalize this idea following [12].

3.1. Theorems

We shall define the system over which we will state the theorems. A proof of these theorems can be found in the appendices of the original paper [12]. The second paper [13] extends these theorems to the case of discrete systems and also provides examples of systems that satisfy the theorems.

Let us first define the system on which we will prove the theorems.

Assumption 1 (System):

We consider a monatomic gas with the interaction

$$U = \sum u(r_{ij}) \quad (3.2)$$

, where r_{ij} is the distance between the i^{th} and j^{th} atoms.

The following assumptions are made about the nature of these interactions':

1. The atoms have a finite impenetrable core of diameter a , so that

$$u(r) = \infty \text{ for } r \leq a \quad (3.3)$$

2. The interaction has a finite range b so that

$$u(r) = 0 \text{ for } r \geq b \quad (3.4)$$

3. $u(r)$ is nowhere minus infinity.

4. Assume that the shape of the container is not pathological, such that its surface area increases slower than $V^{\frac{2}{3}}$.

Condition 2 can be relaxed to include interactions that decay sufficiently fast, such as the Lennard-Jones potential, or the Van der Waals interaction.

Consider a box of volume V containing N indistinguishable atoms of the gas defined above, in contact with a heat and particle reservoir at temperature T and chemical potential μ . The grand partition function of this system is given by

$$\mathcal{Z}(T, V, \mu) = \sum_{N=0}^{N_{\max}} \frac{z^N}{N!} Z(T, V, N) = \sum_{N=0}^M \frac{y^N}{N!} Q(T, V, N) \quad (3.5)$$

where $z = \exp(\beta\mu)$ is the fugacity, $y = \frac{z}{\lambda^3}$, $M = N_{\max}$ and λ is the thermal wavelength. $Z(T, V, N)$ is the canonical partition function, and $Q(T, V, N)$ is the configuration integral defined as

$$Q(T, V, N) = \int \dots \int_v d\tau_1 \dots \tau_N \exp(-\beta U(\boldsymbol{\tau})) \quad (3.6)$$

The pressure and densities can be calculated from the grand partition function in the thermodynamic limit,

$$\begin{aligned} \beta P &= \lim_{V \rightarrow \infty} \left(\frac{1}{V} \right) \ln \mathcal{Z}(T, V, \mu) \\ \rho &= \lim_{V \rightarrow \infty} \left(\frac{1}{V} \right) (z \partial_z \ln \mathcal{Z}(T, V, \mu)) \\ &= \lim_{V \rightarrow \infty} \left(\frac{1}{V} \right) z \frac{\partial y}{\partial z} \frac{\partial \ln(y)}{\partial \ln(y)} \ln \mathcal{Z}(T, V, \mu) \\ &= \lim_{V \rightarrow \infty} \frac{1}{V} \frac{\partial}{\partial \ln(y)} \ln \mathcal{Z}(T, V, \mu) \end{aligned} \quad (3.7)$$

Generally, we exchange the limit $V \rightarrow \infty$ and the derivative $\frac{\partial}{\partial \ln(y)}$, to obtain the equation of state. However, this exchange is only valid if $\ln \mathcal{Z}$ is analytic in y .

Theorem 3.1.1 (Yang-Lee Theorem 1):

For all positive real values of y , $V^{-1} \ln \mathcal{Z}$ approaches, in the limit $V \rightarrow \infty$, a well-defined limit independent of the shape of the volume V . Furthermore, this limit is a continuous and monotonically increasing function of y .

The independence from the shape of the volume V does not imply that this theorem is only valid or fluid phases. One might think that the pressure would change if, say a shearing force is applied to the boundaries of the volume V , changing its shape. As, a result, for solids, this limit should depend on the shape of V . However, the subtlety lies in the fact that the theorem applies in the infinite volume limit. In this limit, the surface effects become negligible compared to the bulk effects, and hence the shape dependence vanishes.

Result 1 (Partition function zeros):

Since the grand partition function \mathcal{Z} is a polynomial in y of degree M , it can be factorized as

$$\mathcal{Z}(T, V, \mu) = \prod_{i=1}^M \left(1 - \frac{y}{y_i} \right) \quad (3.8)$$

Note that the zeros y_i cannot be both real and positive, since all the coefficients of the polynomial are positive (as $Q(T, V, N) > 0$ for all N). Thus, all the zeros lie either in the negative real axis or in the complex plane.

The number of roots increases with the volume V , and in the thermodynamic limit, the distribution of these roots give us complete behavior about the analyticity of $\ln \mathcal{Z}$.

Theorem 3.1.2 (Yang-Lee Theorem 2):

If in the complex y plane, there exists a region R containing a segment of the positive real axis always free of zeros of \mathcal{Z} , then in this region, in the limit $V \rightarrow \infty$,

$$V^{-1} \ln \mathcal{Z}, \frac{\partial}{\partial \ln(y)} V^{-1} \ln \mathcal{Z}, \left(\frac{\partial}{\partial \ln(y)} \right)^2 V^{-1} \ln \mathcal{Z}, \dots \quad (3.9)$$

approach limits that are analytic functions of y . Furthermore, the operators $\frac{\partial}{\partial \ln(y)}$ and $\lim_{V \rightarrow \infty}$ commute in this region,

$$\lim_{V \rightarrow \infty} \frac{\partial}{\partial \ln(y)} V^{-1} \ln \mathcal{Z} = \frac{\partial}{\partial \ln(y)} \lim_{V \rightarrow \infty} V^{-1} \ln \mathcal{Z} \quad (3.10)$$

We now discuss these theorems in the context of phase transitions. The derivatives defined in Theorem 2 do not always approach a limit for all values of y . One can consider the first derivative, relating to density. If the quantity $V^{-1} \frac{\partial}{\partial \ln(y)} \ln \mathcal{Z}$ does not approach a well defined limit, physically this means that the density is not uniquely defined for that value of y . This is the hallmark of a first order phase transition, where two phases coexist at the same pressure and chemical potential, but have different

densities. Thus we need to take a further look at the form of the regions in the complex y plane that are free of zeros. They can be divided into two categories.

3.1.1. No Phase Transition

The roots of $\mathcal{Z} = 0$ do not approach the positive real axis in the thermodynamic limit. Thus there exists a region R containing the positive real axis that is free of zeros. Hence, by Theorem 2, all derivatives of $V^{-1} \ln \mathcal{Z}$ approach analytic limits, and there are no phase transitions. As a result, they are valid to exchange the limit and the derivative, and we can obtain the equation of state. This, the system in consideration is a single phase system for all values of y .

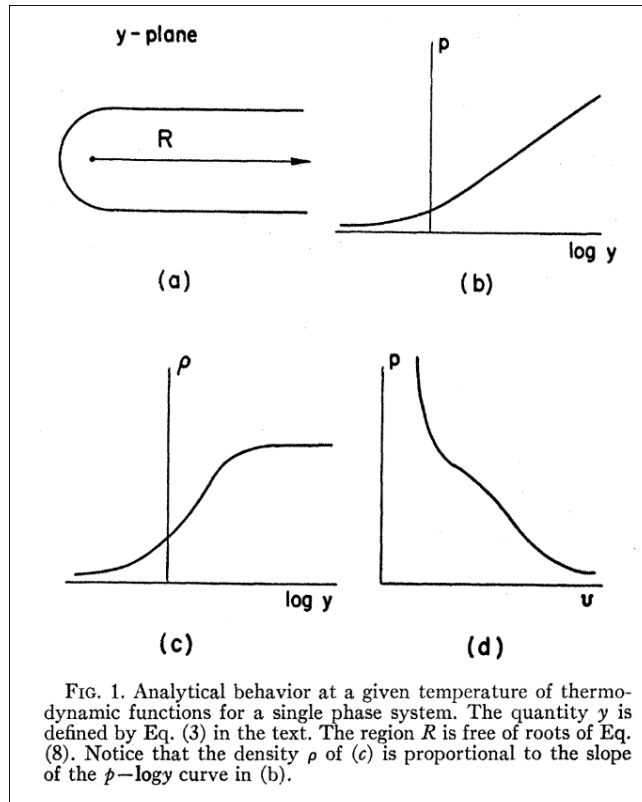


FIG. 1. Analytical behavior at a given temperature of thermodynamic functions for a single phase system. The quantity y is defined by Eq. (3) in the text. The region R is free of roots of Eq. (8). Notice that the density ρ of (c) is proportional to the slope of the p - $\log y$ curve in (b).

Figure 15: Source: [12]

3.1.2. Phase Transition

The roots of $\mathcal{Z} = 0$ approach the positive real axis at some points, say $y = t_1, t_2$ and the regions R_1, R_2, R_3 enclose three root free regions of the positive real axis. Thus, by Theorem 2, all derivatives of $V^{-1} \ln \mathcal{Z}$ approach analytic limits in these regions, and we can exchange the limit and the derivative. However, there is no reason to consider that the limits approached from different regions are the same. In general, they will be different. If they are derivative, we shall observe a jump in the value of the derivative at the boundary between two regions. Physically, this means that the density is not uniquely defined at these points, and we have a first order phase transition. Thus, the system exists in different phases in different regions of y , separated by first order phase transitions at the boundaries.

One can also have a situation where the limits of the first derivatives are the same, but the limits of the second derivatives are different. This would correspond to a second order phase transition.

As different parameters of the system, are varied, the location of the roots in the complex plane also change. As temperature is varied, one might observe that at the roots cease to close in to one of the points on the real line. This temperature would correspond to the critical temperature T_c of the transition $1 \leftrightarrow 2$. One might also observe that at certain values of these parameters, the roots

coalesce at a point on the positive real axis. This would correspond to a triple point, where three phases coexist.

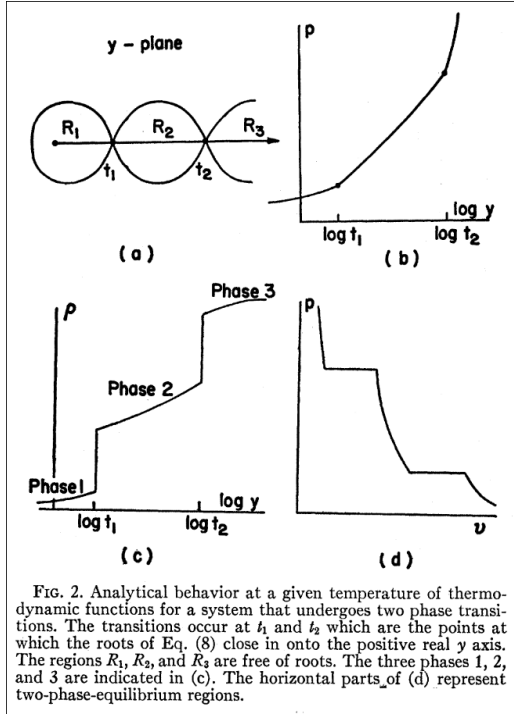


Figure 16: Source: [12]

In the context of the Ising model and lattice gases, Yang and Lee proved the following theorem [13].

Let us consider a system with Ising spins $\sigma_i = \pm 1$ on a lattice, with the applied external magnetic field H . Define the variable $z = \exp(-2\beta H)$. The polynomial \mathcal{P} is defined as

$$\mathcal{P} = \sum_{n=0}^N P_n z^n \quad (3.11)$$

where N is the total number of spins. The coefficients P_n are contributions to the partition function from all configurations with n spins down. This polynomial is similar to the grand partition function of a lattice gas, with z playing the role of fugacity.

Theorem 3.1.2.1 (Yang-Lee Theorem 3): If an interaction u between two gas atoms is such that $u(r) = \infty$ if they both occupy the same lattice site, and $u(r) \leq 0$ otherwise, then all the zeros of the polynomial \mathcal{P} in the complex z plane lie on the unit circle $|z| = 1$.

Note that the condition on the interaction makes no comment about the range of the interaction u , the dimensionality of the lattice, and the size and structure of the lattice. In fact, even the periodicity property of the lattice plays no part at all in the proof. Thus, this theorem is extremely general, and applies to a wide variety of systems.

Lecture 5: Critical exponents of the Van Der Waals Gas.

Lecture 6: Phase Transitions, Critical Exponents and Critical Opalescence.

Lecture 7: Introduction to Mean Field Ising Model

4. Magnetism

The properties of magnetic systems can be studied using statistical mechanics. The simplest model for magnetism is the Ising Model. Before we embark on a mean-field study of the Ising model, let us first draw an analogy between the thermodynamics of fluids and that of magnetic systems. We will try to draw heuristic analogies, between them.

Fluids are characterized by U, V, T, P, N . Suppose our fundamental equation is $U(S, V, N)$. Then,

$$dU = T dS - P dV + \mu dN \quad (4.1)$$

. The extensive variables are S, V, N , and their conjugate intensive variables are $T, -P, \mu$. Now since S can be defined similarly for magnetic systems, as we can use the same statistical definition of entropy. As a result, T can then be defined as the conjugate variable to S . P is the conjugate variable to V . In magnetic systems, we have the additional variables of magnetization M , and applied magnetic field H . Note that magnetic field H scales with the volume of the system, and is thus an extensive variable. The applied magnetic field H is an intensive variable, which is a conjugate variable to M . Thus, we can draw the following analogies:

- Volume $V \rightarrow -M$ Average Magnetization.
- Pressure $P \rightarrow H$ Applied magnetic field.
- Helmholtz Free Energy $F(T, V, N) \rightarrow F(T, M, N)$
- Gibbs Free Energy $G(T, P, N) \rightarrow G(T, H, N)$

The negative in the analogy of V and M arises from the fact that increasing the pressure P decreases the volume V , while increasing the applied field H increases the magnetization M .

4.1. Ising Model

The Ising Model was proposed by Wilhelm Lenz in 1920, and was given to his then PhD student, Ernst Ising. His PhD thesis solved the model in 1 dimension, which he showed does not exhibit a phase transition.

The Ising model Hamiltonian is modeled by simple nearest neighbour interactions. One considers discretizations in both space and in spin space. The discretization in space places the spin on a lattice(classically a square lattice). The Hamiltonian is given by:

$$H\{\sigma\} = -J \sum_{\langle i,j \rangle} \sigma_i \sigma_j - h \sum_i \sigma_i \quad (4.2)$$

- The spins can take the values $\sigma_i \in \{+1, -1\}$.
- The summation $\langle i, j \rangle$ runs over nearest neighbors.
- In 1D, there are no phase transitions. This can be shown perfectly analytically, using two-point spin correlations.

4.2. Mean Field Solution of the Ising Model

The mean field solution is found by considering 0 fluctuations in equilibrium. We approximate the interaction term by noting:

$$(\sigma_i - \langle \sigma_i \rangle)(\sigma_j - \langle \sigma_j \rangle) = 0 \quad (4.3)$$

$$\sigma_i \sigma_j - \langle \sigma_i \rangle \sigma_j - \langle \sigma_j \rangle \sigma_i + \langle \sigma_i \rangle \langle \sigma_j \rangle = 0 \quad (4.4)$$

Using this, one can write,

$$-J \sum_{\langle i,j \rangle} \sigma_i \sigma_j \approx -J \langle \sigma_i \rangle \sum_{\langle i,j \rangle} \sigma_j - J \langle \sigma_j \rangle \sum_{\langle i,j \rangle} \sigma_i + J \langle \sigma_i \rangle \langle \sigma_j \rangle \sum_{\langle i,j \rangle} \quad (4.5)$$

Since the model is translation invariant $\langle \sigma_i \rangle = \langle \sigma_j \rangle = \langle \sigma \rangle$.

Suppose the nearest neighbour summation, can be re-written as,

$$\sum_{\langle i,j \rangle} \approx \frac{\gamma}{2} \sum_{i=1}^N \quad (4.6)$$

This is the second part of the mean-field approximation. This basically states, that the interactions due to the neighbours can be thought of as a mean field over all spins. One can use weaker mean-field approximations like the Bethe-Peierls Approximation.

Using this one can write,

$$\begin{aligned} H_{\text{MF}} &= -J \langle \sigma \rangle \frac{\gamma}{2} \sum_{i=1}^N \sigma_j - J \langle \sigma \rangle \frac{\gamma}{2} \sum_{i=1}^N \sigma_i + J \langle \sigma \rangle \langle \sigma \rangle \frac{\gamma}{2} \sum_{i=1}^N -h \sum_{i=1}^N \sigma_i \\ &= -h_{\text{eff}} \langle \sigma \rangle + J \frac{\gamma}{2} N \langle \sigma \rangle^2 \end{aligned} \quad (4.7)$$

where we denote the effective field as $h_{\text{eff}} = h + J\gamma \langle \sigma \rangle$.

The two approximations, used to solve the model are,

1. There are zero fluctuations.
2. The nearest neighbour interaction can be replaced by a mean field.

One can also solve the mean field model without using the first approximation. See the solution in Appendix. A.1

4.3. Partition Function

First, we try to evaluate the partition function for the mean field Hamiltonian, in the Gibbs canonical ensemble. The free energy functional is given by,

$$A(T, h) = -k_B T \ln Z(T, h) \quad (4.8)$$

Where the partition function is given by:

$$\begin{aligned} Z(T, h) &= \sum_{\{\sigma_i\}} e^{-\beta H_{\text{MF}}} \\ \implies Z(T, h) &= \sum_{\{\sigma_i = \pm 1\}} e^{-\frac{1}{2}\beta N J \gamma \langle \sigma \rangle^2 + \beta h_{\text{eff}} \sum_{i=1}^N \sigma_i} \\ \implies Z(T, h) &= e^{-\frac{1}{2}\beta N J \gamma \langle \sigma \rangle^2} \prod_{i=1}^N \left(\sum_{\sigma_i = \pm 1} e^{\beta h_{\text{eff}} \sigma_i} \right) \\ \implies Z(T, h) &= e^{-\frac{1}{2}\beta N J \gamma \langle \sigma \rangle^2} (2 \cosh(\beta h_{\text{eff}}))^N \end{aligned} \quad (4.9)$$

The Free Energy per spin is:

$$A(T, h) = -k_B T \ln Z = \frac{1}{2} N J \gamma \langle \sigma \rangle^2 - N k_B T \ln(2 \cosh \beta h_{\text{eff}}) \quad (4.10)$$

The magnetization $m = \langle \sigma \rangle$ is:

$$m = -\frac{1}{N} \frac{\partial A}{\partial h} = \beta k_B T \frac{\sinh(\beta(h + J\gamma m))}{\cosh(\beta(h + J\gamma m))} = \tanh(\beta(h + J\gamma m)) \quad (4.11)$$

In the zero field limit $h \rightarrow 0$, we get the transcendental equation for magnetization:

$$m = \tanh(\beta J \gamma m) \quad (4.12)$$

Let $x = \beta J \gamma m$, then:

$$\frac{k_B T}{J\gamma} x = \tanh(x) \Rightarrow \frac{T}{T_c} x = \tanh(x) \quad (4.13)$$

Where the critical temperature is

$$T_c = \frac{J\gamma}{k_B} \quad (4.14)$$

4.4. Critical Exponents and Behavior

Near the critical point $t = \frac{T-T_c}{T_c} \rightarrow 0$:

- Specific Heat: $C \sim t^{-\alpha}$
- Magnetization: $m \sim (-t)^\beta$
- Susceptibility: $\chi \sim t^{-\gamma}$
- Equation of State: $H \sim |M|^\delta$ (at $T = T_c$)

In Mean Field Theory, $\beta = \frac{1}{2}$. Experimental data (e.g., MnF_2) shows $\beta \approx 0.33$, and 2D Ising gives $\beta = \frac{1}{8}$ due to conformal symmetry.

4.5. Phase Diagrams and Hysteresis

At $h = 0$, there is a second-order phase transition at T_c . At $h \neq 0$, there is no transition, but a crossover. Below T_c , changing h from positive to negative leads to a first-order transition with hysteresis.

4.6. Bragg-Williams Approximation

Using the canonical ensemble for a Lattice Gas (N_+ up, N_- down):

$$m = \frac{N_+ - N_-}{N} \Rightarrow \frac{N_+}{N} = \frac{1}{2}(m + 1) \quad (4.15)$$

Entropy from Stirling's approximation:

$$\frac{S}{Nk_B} \approx \ln 2 - \left[\frac{1+m}{2} \ln(1+m) + \frac{1-m}{2} \ln(1-m) \right] \quad (4.16)$$

Energy (ignoring correlations):

$$U = -\frac{NJm^2\gamma}{2} - Nhm \quad (4.17)$$

Minimizing $F = U - TS$ with respect to m yields the same self-consistency equation:

$$h = \frac{\partial F}{\partial M} \Rightarrow m = \tanh(\beta(h + J\gamma m)) \quad (4.18)$$

References

- [1] F. Reif, *Fundamentals of Statistical and Thermal Physics*. New York: McGraw-Hill, 1965.
- [2] M. Kardar, *Statistical Physics of Particles*. Cambridge: Cambridge University Press, 2007.
- [3] R. K. Pathria and P. D. Beale, *Statistical Mechanics*, 3rd ed. Elsevier, 2011.
- [4] H. B. Callen, *Thermodynamics and an Introduction to Thermostatistics*, 2nd ed. John Wiley & Sons, 1985.
- [5] S. Seth, “Advanced Statistical Physics Lecture Notes.” [Online]. Available: <https://lonewolf1304.github.io/>
- [6] H. E. Stanley, *Introduction to Phase Transitions and Critical Phenomena*. Oxford University Press, 1971.
- [7] E. M. Prodanov, “Mathematical analysis of the van der Waals equation,” *Physica B: Condensed Matter*, vol. 640, p. 414077, Sept. 2022, doi: [10.1016/j.physb.2022.414077](https://doi.org/10.1016/j.physb.2022.414077).
- [8] V. K. L. Mer, “Nucleation in Phase Transitions.,” *Industrial & Engineering Chemistry*, vol. 44, no. 6, pp. 1270–1277, June 1952, doi: [10.1021/ie50510a027](https://doi.org/10.1021/ie50510a027).
- [9] “Lecture: Supercooling and Nucleation..” [Online]. Available: https://ethz.ch/content/dam/ethz/special-interest/chab/icb/shih-lab-dam/documents/IEM-lecture/Lecture_2024/Notes_2024/Lecture_5_2024.pdf
- [10] M. Deserno, “Legendre transforms - andrew.cmu.ed.” [Online]. Available: <https://www.andrew.cmu.edu/course/33-765/pdf/Legendre.pdf>
- [11] R. K. P. Zia, E. F. Redish, and S. R. McKay, “Making Sense of the Legendre Transform,” 2008, doi: [10.48550/ARXIV.0806.1147](https://arxiv.org/abs/0806.1147).
- [12] C. N. Yang and T. D. Lee, “Statistical theory of equations of state and phase transitions. I. theory of condensation,” *Phys. Rev.*, vol. 87, no. 3, pp. 404–409, Aug. 1952.
- [13] T. D. Lee and C. N. Yang, “Statistical theory of equations of state and phase transitions. II. Lattice gas and Ising model,” *Phys. Rev.*, vol. 87, no. 3, pp. 410–419, Aug. 1952.
- [14] E. of Mathematics, “Viète theorem,” *Encyclopedia of Mathematics*, 2001, Accessed: Oct. 15, 2023. [Online]. Available: https://encyclopediaofmath.org/wiki/Vi%C3%A8te_theorem

Appendix 1: Alternate Mean field Solution

One can solve Eq. (4.7) without using the first approximation, which is the approximation of 0 fluctuations. We will outline the solution by Baxter. This model is pretty nice because we can graphically see why the phase transition takes place.

A.1. The Mean Field Hamiltonian

The mean field Hamiltonian, interestingly, does not feature the classic nearest neighbor interactions in the Ising Model. Suppose each spin site on a lattice of N sites, has q neighbors,(2d for a d dimensional Ising Model). The total field acting on that is given by,

$$H + J \sum_{\{j\}} \sigma_j \quad (1.1)$$

where the summation is over the q neighbors of the spin site. For the mean field the interactions over all other $N - 1$ sites, averaged and then amplified over the number of neighbors q . The field for a spin at site i is given by

$$H + (N - 1)^{-1} q J \sum_{j \neq i} \sigma_j \quad (1.2)$$

where the sum is taken over all $N - 1$ sites. The Hamiltonian is thus given by,

$$\mathbb{H}(\{\sigma\}) = -\frac{qJ}{N-1} \sum_{i,j} \sigma_i \sigma_j - H \sum_i \sigma_i \quad (1.3)$$

where the first sum is over all the $\binom{N}{2} = \frac{1}{2}N(N-1)$ distinct pairs. There is an unphysical property here. The strength of coupling between spins depends on the number of spin sites. However, we can get some proper thermodynamic properties from the model. This analytically solvable model also exhibits phase transitions. The total magnetization is defined as

$$M = \sum_{j=1}^N \sigma_j \quad (1.4)$$

Let there be r down spins, then the number of up spins is given by $N - r$. The total magnetization for r down spins is given by $M_r = N - 2r$. Note,

$$\begin{aligned} M_r^2 &= \sum_{i,j} \sigma_i \sigma_j = \sum_{i=1}^N \sigma_i^2 + \sum_{i \neq j} \sigma_i \sigma_j \\ &\Rightarrow \sum_{i \neq j} \sigma_i \sigma_j = M_r^2 - N = (N - 2r)^2 - N \end{aligned}$$

A small note here, here the sum distinguishes (i, j) and (j, i) , but the sum in the Hamiltonian only takes into account distinct pairs. The mean field Hamiltonian can be rewritten in terms of the magnetization and indexed by the number of down spins r .

$$\begin{aligned} \mathbb{H}_r &= -\frac{qJ}{N-1} \sum_{i,j} \sigma_i \sigma_j - H \sum_i \sigma_i = -\frac{qJ}{N-1} [M_r^2 - N] - HM_r \\ &= -\frac{qJ}{2(N-1)} [(N - 2r)^2 - N] - H(N - 2r) \end{aligned} \quad (1.5)$$

A.2. Magnetization and Free Energy

The partition function is now expressed as,

$$\begin{aligned} Z_N &= \sum_{r=0}^N c_r \text{ where} \\ c_r &= \binom{N}{r} \exp\left(\frac{q\beta J}{2(N-1)}[(N-2r)^2 - N] + \beta H(N-2r)\right) \end{aligned} \tag{1.6}$$

The properties of c_r can be analyzed using $d_r = \frac{c_{r+1}}{c_r}$. To motivate this expression, we consider this to characterize the sets where c_r is increasing and c_r is decreasing. Using that we can determine r where c_r takes the maximum value and some Laplace Method approximation can be applied. The graphs of these c_r and d_r will also be provided, which also helps in motivating whatever algebraic jugglery we might indulge in here. The expression for d_r is given by,

$$\begin{aligned} d_r &= \frac{c_{r+1}}{c_r} = \frac{\binom{N}{r+1} \exp\left(\frac{q\beta J}{2(N-1)}[(N-2r-2)^2 - N] + \beta H(N-2r-2)\right)}{\binom{N}{r} \exp\left(\frac{q\beta J}{2(N-1)}[(N-2r)^2 - N] + \beta H(N-2r)\right)} \\ &= \frac{N-r}{r+1} \exp\left(-2\beta qJ\left(1 - \frac{2r}{N-1}\right) - 2\beta H\right) \\ &= A_H \frac{N-r}{r+1} \exp\left(-2\beta qJ\left(1 - \frac{2r}{N-1}\right)\right) \end{aligned} \tag{1.7}$$

Let us consider a continuous extension to this for non-natural r . Let $\varphi(x)$ be a function such that for $r = \{0, 1, \dots, N\}$, we have $\varphi(r) = d_r$. Let's ignore the initial A_H factor, since it's just a scaling factor which is the same for all x . A natural choice for this is given by,

$$\varphi(x) = \frac{N-x}{x+1} \exp\left[-2\beta qJ\left(1 - \frac{2x}{N-1}\right)\right] \tag{1.8}$$

The derivative of the function should be able to tell us something about the domains where the function rises and where it dips. Let us denote $\eta = 2\beta qJ$ for ease of algebra

$$\varphi'(x) = -\frac{2\eta x^2 + 2\eta(1-N)x + (N^2 - 2\eta N - 1)}{(N-1)(x+1)^2} \exp\left(-\eta\left(1 - \frac{2x}{N-1}\right)\right) \tag{1.9}$$

We can just focus on the quadratic term in the derivative. The other terms, namely the exponential and the denominator are always zero. The zeros of the quadratic define maxima and minima of the function. The function thus can attain either one or two stationary points. When the function has complex roots, we just get a monotonically decreasing function over the whole domain. Thus, d_r is a monotonically decreasing function. The quadratic term has complex roots when,

$$\eta \leq \frac{2(N-1)}{N+1} \implies q\beta J \leq \frac{N-1}{N+1} \tag{1.10}$$

As we shall see later, this condition will determine the critical temperature. The other case can be that the quadratic term has two positive or two negative roots, using Vieta's Theorem [14]. The roots are given by

$$x_{\pm} = \frac{\eta(N-1) \pm \sqrt{\eta^2(N-1)^2 - \eta(N^2 - 2\eta N - 1)}}{2\eta} \tag{1.11}$$

Since x_+ is positive, both roots must be positive. Thus, we have two cases, one where the function decreases monotonically, and one where it has two positive roots. Let us examine the case, where there is no root, $qJ \leq k_B T$. Note that for this condition the function d_r starts somewhere greater than 1 and goes to 0 when $r = N$. Thus, there is one point where the function $\varphi(x)$ crosses the line $y = 1$. Thus, in the discrete version of d_r , there is some $r_o \in \{0, \dots, N\}$ such that we obtain,

$$\begin{aligned} d_r > 1 &\quad r = \{0, 1, \dots, r_o - 1\} \\ d_{r_o} \geq 1 &\quad r_o \\ d_r < 1 &\quad r = \{r_o + 1, \dots, N\} \end{aligned} \tag{1.12}$$

Thus, there is a maximum value of c_r which it attains at some point r_o . We shall exploit this later when we use a Saddle point approximation on our problem. When the case for double roots are considered, assuming you take high enough N for a given η , we will obtain three points where $\varphi(x) = 1$. This fact can be easily seen if you observe the fact that the two points where the derivative of $\varphi(x)$ is symmetric with respect to $x = (N - 1)/2$. At that point x , the derivative of $\varphi(x)$ is greater than or equal to zero. If it is equal to zero, it corresponds to the repeated root condition and that also means there is only 1 point where $\varphi(x)$ crosses 1. If the slope is positive, then $\varphi(x_+)$ and $\varphi(x_-)$, are above and below 1 respectively. Thus, the function d_r crosses the line $y = 1$ three times. The graph of $\varphi(x)$ and d_r has been plotted below. Three graphs have been plotted, one where there are no stationary points, one where there is one stationary point and one where there are two. Our extremely tedious and completely unmotivated analysis has matched with computational results.

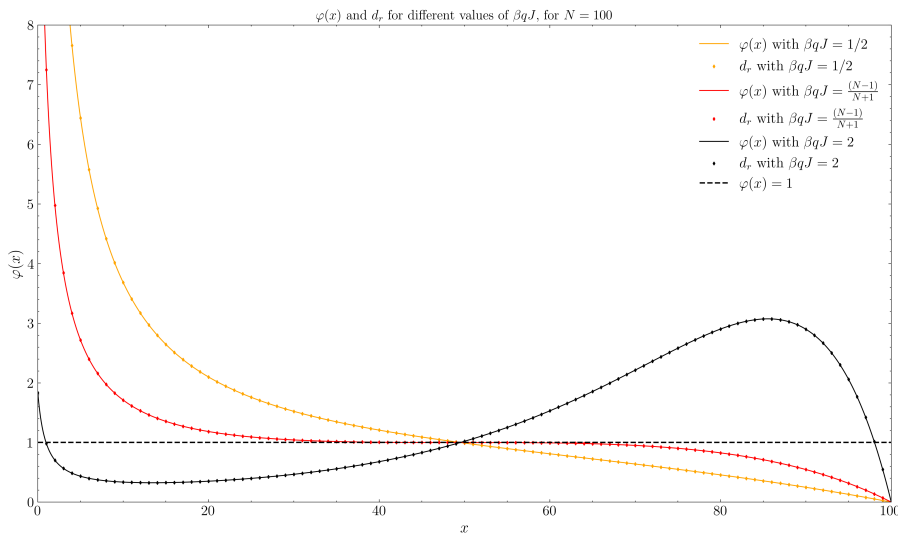


Figure 17: The dependence of $\varphi(x)$ and d_r on $q\beta J$

Before we move on to the critical temperature and the graphs of c_r , the magnetization needs to calculated. The average magnetization per site is then defined to be,

$$m = N^{-1} \langle M \rangle = \left\langle 1 - \frac{2r}{N} \right\rangle = Z^{-1} \sum_{r=0}^N \left(1 - \frac{2r}{N} \right) c_r \quad (1.13)$$

The height of the peak at c_{r_o} scales with N , and the width of the peak scales with $N^{1/2}$. So we can say that the maximum contribution of the sum is given by the maximum summand. Let us define another function, which we will motivate after we introduce the function.

$$d_r = \frac{c_{r+1}}{c_r} = \psi \left(1 - \frac{2r}{N} \right) \quad (1.14)$$

where we can manipulate the general continuous function $\psi(x)$, where $-1 < x < 1$, to remove all dependence on r and N . For this next step assume that we have $N \gg 1$, i.e. a large number of sites. The functional form is given by,

$$\begin{aligned}
\psi\left(x = 1 - \frac{2r}{N}\right) &= \frac{N-r}{r+1} \exp(-2\beta qJx - 2\beta H) \\
\Rightarrow \psi\left(x = 1 - \frac{2r}{N}\right) &= \frac{1+1-\frac{2r}{N}}{1+\frac{2}{N}-(1-\frac{2r}{N})} \exp(-2\beta qJx - 2\beta H) \\
\Rightarrow \psi(x) &= \frac{1+x}{\frac{2}{N}+1-x} \exp(-2\beta qJx - 2\beta H) \\
\Rightarrow \psi(x) &\approx \frac{1+x}{1-x} \exp(-2\beta qJx - 2\beta H)
\end{aligned} \tag{1.15}$$

Note that $-1 < x < 1$. We are looking for the point r_o where c_r attains the maximum value at c_{r_o} . If N is large enough, c_{r_o+1} and c_{r_o} are close enough that we look for the point where $d_{r_o} = 1 = \psi(x_o = 1 - \frac{2r_o}{N})$. Note that the value of x_o only depends on βqJ and βH , and does not depend on N at large N . The average magnetization can then be given by,

$$\begin{aligned}
m &= \lim_{N \gg 1} Z^{-1} \sum_{r=0}^N \left(1 - \frac{2r}{N}\right) c_r \\
&= \lim_{N \gg 1} Z^{-1} \sum_{r=0}^N x_r c_r \\
&= x_{r_o} \frac{c_{r_o}}{c_{r_o}}
\end{aligned} \tag{1.16}$$

Thus, $\psi(m) = 1$. Again our average magnetization is Thus we can find the solution of m , in the form of a transcendental equation. The average magnetization m is given by,

$$\begin{aligned}
\frac{1+m}{1-m} &= \exp(2\beta qJm + 2\beta H) \\
\Rightarrow m(\beta) &= \frac{\exp(\beta qJm + \beta H) - \exp(-\beta qJm - \beta H)}{\exp(\beta qJm + \beta H) + \exp(-\beta qJm - \beta H)} \\
\Rightarrow m(\beta) &= \tanh(\beta qJm + \beta H)
\end{aligned} \tag{1.17}$$

The free energy per site is calculated for the system before we move onto the critical behavior and temperature for the model. The free energy per site, for infinitely large systems is given by,

$$-\beta f = \frac{1}{2} \ln\left(\frac{4}{1-m^2}\right) - \frac{1}{2} qJ\beta m^2 \tag{1.18}$$

Result 2 (Free Energy and Magnetization of the Mean Field model):

The free energy per site is given by

$$-\beta f = \frac{1}{2} \ln\left(\frac{4}{1-m^2}\right) - \frac{1}{2} qJ\beta m^2 \tag{1.19}$$

and the average magnetization is given by

$$m(\beta) = \tanh(\beta qJm + \beta H) \tag{1.20}$$

The free energy cannot be expressed in just in terms of H without dependence on m . So we look at the behavior of m as a function of H .

A.3. Critical Point

We can obtain the H as a function of m and then rotate the axes to find how m varies with H .

$$H(\beta) = qJ \left(m + \frac{1}{q\beta J} \tanh^{-1}(M) \right) \quad (1.21)$$

We can plot this and then reverse the graph to easily visualize the plot of m versus H and see how we get a phase transition. Furthermore, we know that when $T > \frac{qJ}{k_B}$, there is only one solution to $d_r = 1$, the graph is plotted below. There is no spontaneous magnetization, which we expect.

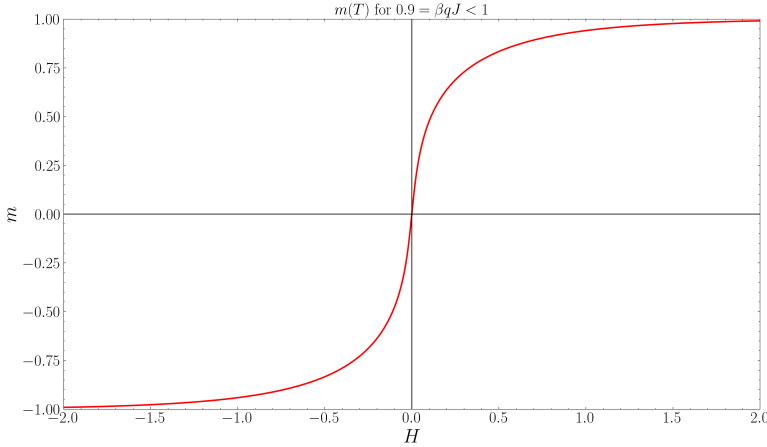
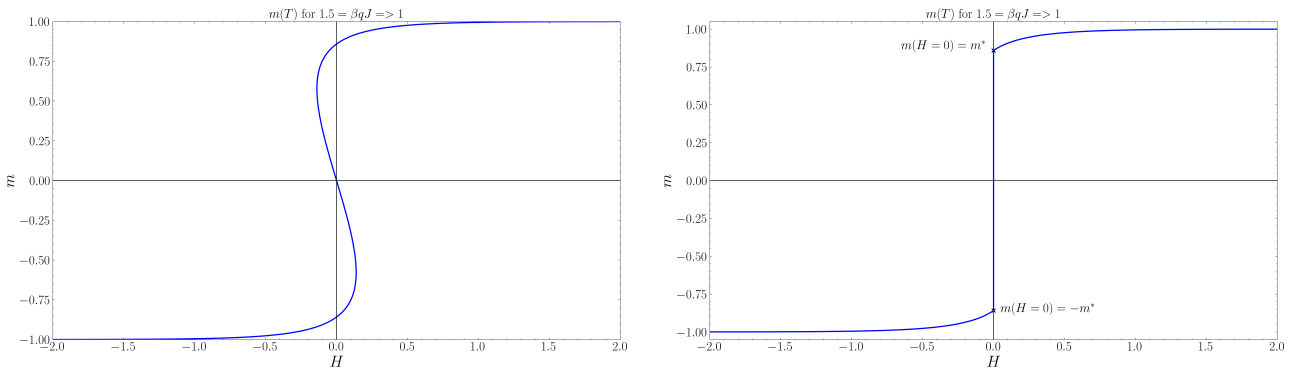


Figure 18: At higher temperatures, the graph of magnetization versus the applied magnetic field

At lower temperatures, $T < \frac{qJ}{k_B}$, the graph is quite frankly, ridiculous, because for a specific applied magnetic field H , there is a region, where 3 values of magnetization are possible. This apparent oddity comes from our approximation. In this lower temperature regime, there are three solutions to $d_r = 1$, as we have seen in the graph before. This directly follows the 2 stationary points of d_r . These correspond to 3 stationary points in c_r . Instead of choosing local minima the maximum contribution comes from the absolute maximum. So the wrong solutions need to be rejected.



(a) Complete solution of m vs H .

(b) After rejection of idiotic solutions.

Figure 19: The complete and corrected graph of magnetization vs applied magnetic field.

A nice thing can be noted if we plot, for a given qJ and $T < \frac{qJ}{k_B}$, the graph of c_r and for two values $H = -h$ and $H = h$. We observe in the graph of c_r there are 2 maxima and 1 minima. One maximum is the absolute maximum when $H = h$ and the other maxima is attains the maximum value when $H = -h$. This is the core property which causes the phase transition to occur for this model. The

maximum value of c_{r_o} comes for different values of r_o if the limit of magnetic field is taken $H \rightarrow 0-$ and $H \rightarrow 0+$. The graph of c_r vs r for a low enough temperature is plotted below for small values $H = -h, h$. From this we determine the critical temperature to be,

$$T_c = \frac{qJ}{k_B} \quad (1.22)$$

Here are some supplemental graphs to cement the fact that the peak scales with N and the width of the peak scales as $N^{\frac{1}{2}}$, for both $T < T_c$ and $T > T_c$. One can see how the probabilities in the different phases lead to a symmetry breaking.

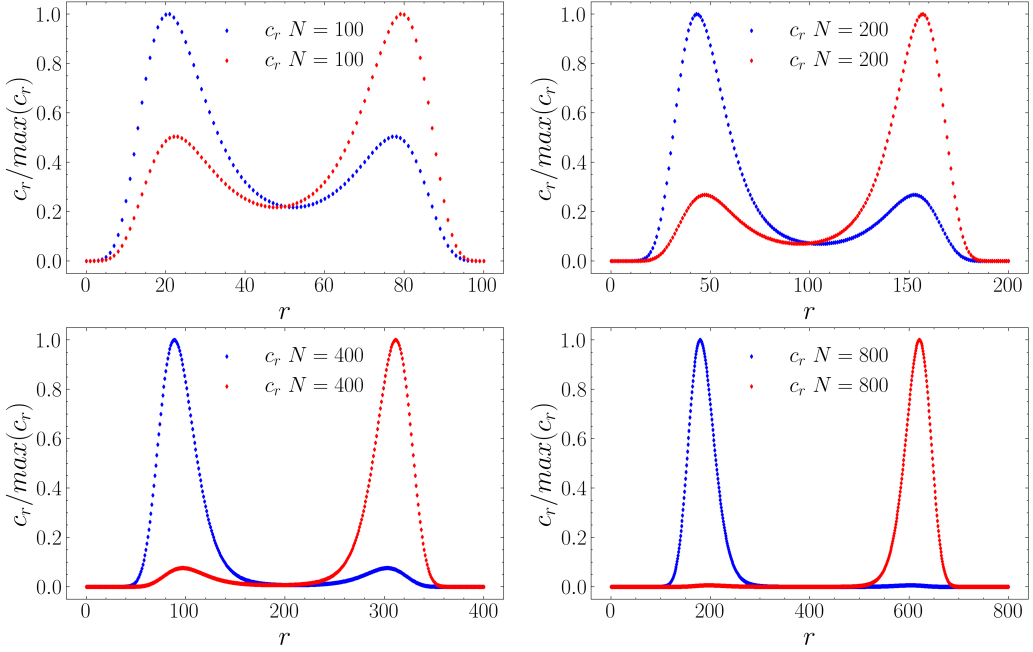


Figure 20: The graph of c_r vs r for $T < T_c$ for different values of $N = 100, 200, 400, 800$

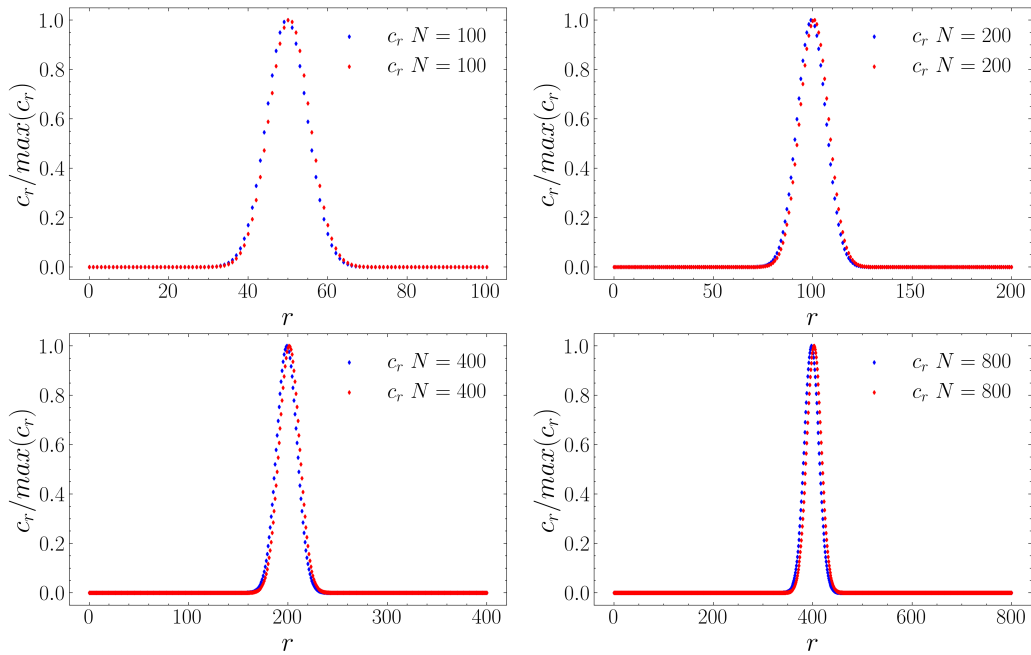


Figure 21: The graph of c_r vs r for $T > T_c$ for different values of $N = 100, 200, 400, 800$